EVALUATION OF ENVIRONMRNTAL FACTORS AFFECTING STEEL CORROSION IN CONCRETE EXPOSED TO PORT AND HARBOR MARINE CONDITIONS

(Translation from JCI Concrete Research and Technology, Vol. 13, No.2, May 2002)




Hidenori HAMADA Hiromichi MATSUSHITA Nobuaki OTSUKI Tsutomu FUKUTE

Damage to RC structures by chloride attack in a marine environment is a common problem in Japan. Consequently, there is considerable need for the development of a repair design methodology for damaged structures as well as a durability oriented design methodology for new structures. An essential component of such design methodologies will be a quantitative method of evaluating the environmental conditions to which a structure is subjected. To date, however, the amount of research data accumulated is insufficient. In this study, small mortar specimens are exposed for two years at nineteen ports located from Hokkaido to Okinawa. Using the test result, analysis is carried out and the environmental factors affecting deterioration of mortar specimens is discussed quantitatively. From this experimental series, several environmental factors are selected as key factors affecting steel corrosion in mortar and mortar deterioration.

Key Words *: Port and harbor RC structures, chloride attack, steel corrosion, marine environment*

Hidenori HAMADA is Head of Materials Division, Port and Airport Research Institute, Independent Administrative Institution, Japan. He obtained his D. Eng. from Kyushu University. His research topics are related to port and airport construction materials.

Hiromichi MATSUSHITA is Professor of Department of Civil Engineering, Faculty of Engineering, Kyushu University, Japan. He obtained his D. Eng. from Kyushu University. His research topics are related to all areas of construction materials.

Nobuaki OTSUKI is Professor, Department of International Development Engineering, Tokyo Institute of Technology, Japan. He obtained his D. Eng. from Tokyo Institute of Technology. His research topics are related to durability and rehabilitation of all kinds of concrete structures.

Tsutomu FUKUTE is Professor of Department of Civil and Environmental Engineering, Toyo University, Japan. He obtained his D. Eng. from Nagoya University. His research topics are related to maintenance and lifecycle management of all kinds of infrastructures.

1. INTRODUCTION

As a nation surrounded by the sea, Japan has pursued economic growth and human development by trading with other countries using marine transport. Historically, most Japanese cities have been associated with nearby seaports, and port facilities are generally constructed of steel and concrete in the form of RC (Reinforced Concrete) structures. Since the 1970s, chloride attack has been recognized as a major factor causing the deterioration of many port and harbor RC structures [1][2][3]. Among concrete port and harbor components, the upper concrete deck (consisting of beams and slabs) is usually the most seriously affected by chloride attack. Typical chloride-induced signs of deterioration are rust stains, cracking of the concrete surface, and spalling of the concrete cover.

In the case of inland structures, chloride attack often results from initial chloride ions in the fresh concrete, which may be supplied by unwashed sea-sand or chlorine-containing chemical admixtures. However, port and harbor concrete structures are subject to a marine environment that exposes them to seawater splashing and salt-laden air. Under such severe conditions, an abundance of chloride ions is able to penetrate the hardened concrete [4]. Consequently, different countermeasures are needed to protect port and harbor concrete structures against chloride-induced deterioration.

Generally, environmental conditions have a great bearing on steel corrosion. That is, even an identical steel material will suffer different corrosion rates and corrosion trends under different environmental conditions. In order to establish methodologies for durability-oriented design and repair design, it is essential to develop a method of quantitatively evaluating the environmental conditions to which a structure is exposed. However, there has been insufficient study of this topic, and accumulated information on environmental conditions is very limited. This research program was planned and implemented to correct this situation.

In the study, relatively small cylindrical specimens of mortar were exposed at nineteen ports for a period of two years. After two years of exposure, characteristics of the specimens were tested and the results were analyzed. This paper summarizes the test procedure and discusses the effect of climate and marine conditions on steel corrosion in the specimens on the basis of the analysis.

2. TEST PROCEDURE AND RESULTS

2.1 Formulation of Corrosion Rate and Amount of Corrosion

Basically, the amount of corrosion is calculated according to Equation (1).

$$W_{corr} = \int_{t_1}^{t_2} \sigma \cdot dt \qquad (1)$$

Here, W_{corr} is the amount of corrosion, σ is the corrosion rate, t_1 is the time at which corrosion initiates, and t_2 is the time at which the corrosion amount is to be calculated. From Equation (1), it is clear that the amount of corrosion cannot be measured directly using an electrochemical technique. On the other hand,

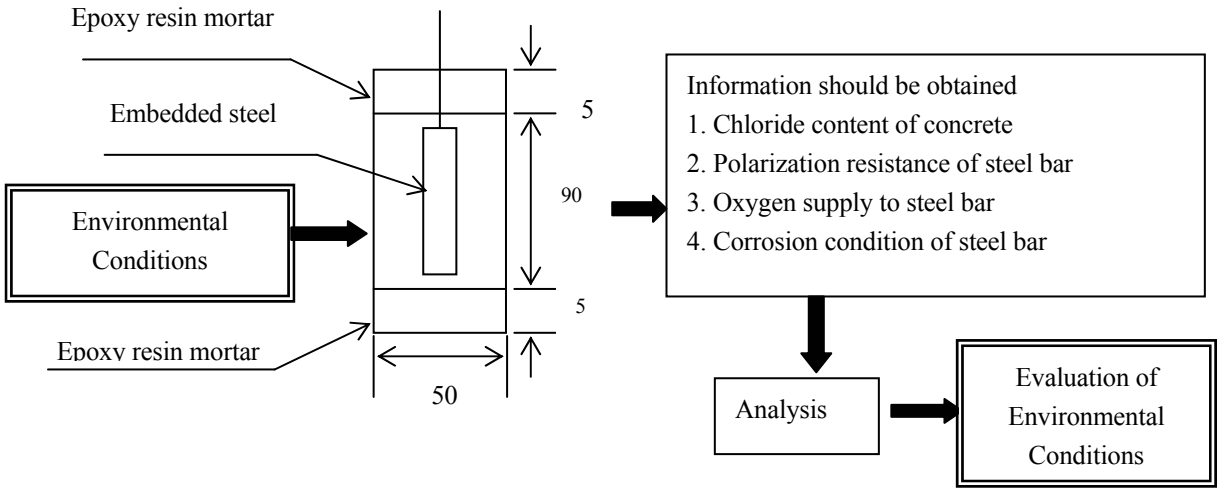

Fig. 1 Fundamental basic evaluation of climatic and marine conditions and outlines of mortar specimen

the corrosion rate can be measured electrochemically.

2.2 Method of Evaluating Climate and Marine Conditions

a) Fundamental basis

The fundamental basis for evaluation of the mortar specimens is explained in Fig.1. Cylindrical specimens embedded with a steel bar were exposed in actual port locations for two years. After two years of exposure, characteristic changes to the cylinder specimens were measured. By analyzing the test results, the effect of climate and marine conditions on the specimens was evaluated. The fundamental theory behind the tests is that, first, a specimen absorbs the effectiveness of environmental conditions during the exposure period, and second that the effect can be evaluated by carrying out several tests on the specimen after exposure.

b) Definition of "system", "environment", and "boundary"

It is necessary to clearly define the terms used in this analysis. The "system" includes any attached chloride, so the "boundary" is defined as an assumed surface just outside the specimens' mortar surface. The "environment" is then defined as everything outside of this assumed surface.

c) Evaluation of climate and marine conditions

Equation (1) comprises two parameters: corrosion rate and duration of corrosion. For steel bars embedded in concrete, the time at which corrosion initiates is mainly governed by the rate of chloride diffusion into the concrete. Further, corrosion rate is mainly governed by passivity conditions at the steel surface and the rate of oxygen supply to the concrete. Information on these three parameters is obtained from the exposed mortar specimens. First, the chloride content of the mortar was measured and the chloride diffusion coefficient calculated. Based on this chloride diffusion coefficient, the corrosion initiation time was calculated, and also the duration of corrosion was obtained. To obtain information on passivity conditions, the polarization resistance was measured. Further, in order to obtain information on the rate of oxygen diffusion into the mortar, potential step measurements were carried out. The details of these various measurements are explained in a later section. In the second stage of the research, the interrelationships

between these test results and climate and marine conditions at each port were investigated. Based on this investigation, the effect of climate and marine conditions on the duration of corrosion, passivity conditions at the steel surface, and the rate of oxygen supply are discussed.

2.3 Outline of Exposure Ports and Method of Exposure

Figure 2 shows the locations of the ports at which mortar specimens were exposed. These consist of eighteen real ports and one artificial exposure site at the Port and Airport Research Institute (PARI). The exposure test began in October 1989. In March 1990, October 1990, and October 1991, specimens were taken from the exposure sites and tested for the 6-month, 1-year, and 2-year test, respectively. Exposure was on a wharf structure at each port. Specimens in the "splash zone" were located at a point 50 cm above high water level (HWL). Those in the "tidal zone" were at mean water level (MWL). Those in the "submerged zone" were 1 m below low water level (LWL). Those in the "land zone" were exposed to sea air, but were not directly exposed to seawater splashing.

Fig. 2 Location of exposure ports

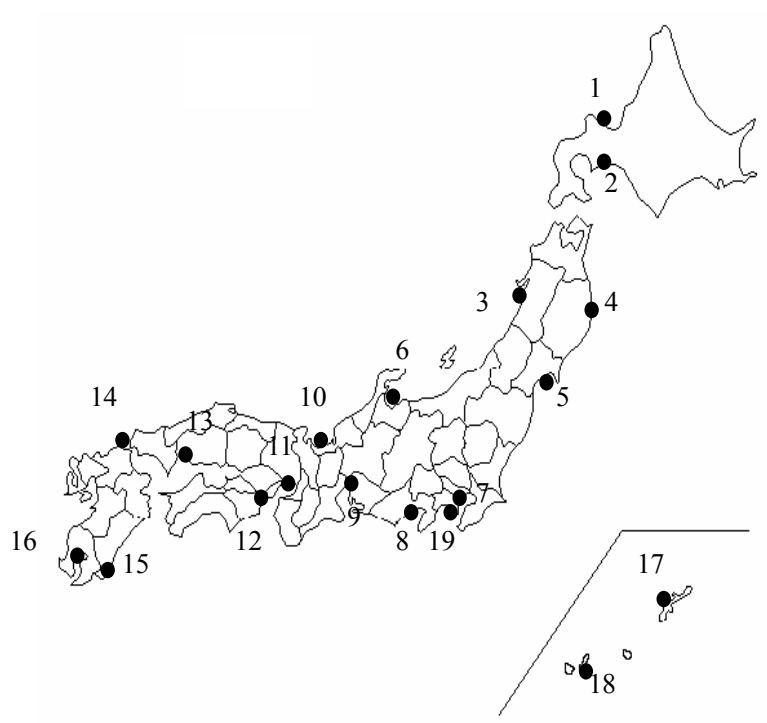

1 Otaru
2 Tomakomai
3 Akita
4 Miyako
5 Shiogama
6 Fushiki-Toyama
7 Yokohama
8 Shimizu
9 Nagoya
10 Maizuru
11 Kobe
12 Komatsujima
13 Hiroshima
14 Kitakyushu
15 Aburatsu
16 Kagoshima
17 Naha
18 Ishigaki
19 PARI

2.4 Climatic and Marine Conditions at Exposure Ports

a) Climate at exposure ports [5]-[28]
The following climate data was collected for the duration of the tests: 1) Monthly average temperature, 2) Monthly average of daily highest temperature, 3) Monthly average humidity, 4) Monthly average wind velocity, 5) Monthly maximum wind velocity, 6) Monthly sunshine hours, and 7) Monthly rainfall.
b) Seawater composition at exposure ports

Table 1 gives the items for which the seawater at each port was analyzed. Chemical analysis was carried out on samples of about 1 liter taken from the surface in the vicinity of the exposure site. Sampling of seawater was carried out in January 1991, April 1991, July 1991, and October 1991, and the average of the four data points was used in the later analysis.

Table 1 Seawater analysis items and methods

Item	Method
Specific gravity	JIS K 2249 Test methods for density of crude oil and petroleum products, and petroleum measurement tables based on a reference temperature of 15 centigrade
pH, Na, K, Ca, Cl^-, SO_4, Mg	JIS K 0102 Test methods for industrial waste water

c) Wave conditions at exposure ports [29][30][31]

From among the nineteen exposure ports, data on wave conditions were collected at Tomakomai, Akita, Miyako, Kobe, Aburatsu, Kagoshima, and Naha. Of the various wave data, wave height and frequency are thought to be most important. In this study, maximum wave height ($H_{1/3}$ max) and average wave height are considered. Frequency is expressed as the inverse of wave period. Using these values, the value of wave height divided by wave period (H/T) was used as a parameter for the effect of wave conditions.

2.5 Outline of Mortar Specimens

The mortar specimens were cylinders measuring 50 mm in diameter and 100 mm in height. The mortar portion was 90 mm in height, and both ends were protected with a layer of epoxy resin mortar measuring 5 mm in thickness. The epoxy resin mortar consisted of epoxy resin 25% and Toyoura standard sand 75% by weight. Round steel bar measuring 9 mm in diameter and 50 mm in length was embedded in the center of each mortar specimen. Leads were connected to the ends of the steel bar, with the connection covered in epoxy resin to prevent current leakage during electrical measurements. The materials used for the mortar were Ordinary Portland Cement (density: 3.16g/cm^3, specific surface area: 3180 cm^2/g), Toyoura standard sand, and ordinary tap water. The mix proportion consisted of cement, sand, and water in the ratio 1.0 : 1.8 : 0.5. The compressive strength and bending strength of the mortar at 7 days were measured as 37.7 N/mm^2 and 7.6 N/mm^2, respectively. Table 2 gives the physical properties and chemical composition of the cement. Table 3 gives the chemical composition of the steel bar.

Table 2 Physical properties and chemical composition of cement

Density (g/cm^3)	Specific surface area (cm^2/g)	MgO (%)	SO_3 (%)	Ig. Loss (%)
3.16	3180	1.4	2.1	0.7

Table 3 Chemical composition of steel bar

C (%)	Si (%)	Mn (%)	P (%)	S (%)
0.12	0.20	0.49	0.020	0.021

2.6 Test Items, Methods, and Results

a) Test items

Tests carried out on the mortar itself consisted of 1) chloride ion content and 2) electric resistance. The measurements made on the embedded steel bar were 1) polarization resistance, 2) potential-step measurements, and 3) corroded area. For each of these test items, two specimens were used and the average of the two data points was used in subsequent analysis.

b) Chloride ion content

Mortar samples were taken from two locations on each specimen, one on the surface (0 to 5 mm in depth) and the other around the steel bar (about 20 mm below the surface). The collected mortar particles were ground into a powder and the acid-soluble chloride ion content was measured according to the JCI method [32]. The chloride content is expressed here in weight percent versus cement.

c) Calculation of chloride ion diffusion coefficient

Based on the measured chloride contents of the mortar after exposure durations of 6 months, 1 year, and 2 years, the diffusion coefficient is calculated. The calculation is carried out according to the theory of heat transfer in an infinitely long cylindrical bar [33]. In this study, the chloride ion distribution over the cross section is expressed as Equation (2).

$$\frac{\partial C}{\partial t} = \kappa\left(\frac{\partial^2 C}{\partial r^2} + \frac{1}{r}\frac{\partial C}{\partial r}\right) \qquad (2)$$

Here, C: chloride ion content at (r,t), k: diffusion coefficient, t: exposure duration, and r: distance along radius from center of cross section. The solution to Equation (2) can be expressed as Equation (3):

$$C = C_0 - 2C_0\sum_{\alpha}\frac{1}{\alpha J_1(\alpha)}e^{-\frac{\alpha^2}{a^2}\kappa t}J_0\left(\frac{\alpha}{a}r\right) \qquad (3)$$

Here, C_0: surface chloride content of mortar specimen and a: radius of cylindrical specimen (= 2.5 cm). The function Jn(x) in Equation (3) is the n-th dimensional first Bessels' function, defined as indicated by Equation (4).

$$J_n(x) = \sum_{k=0}^{\infty}\frac{(-1)^k}{k!\Gamma(n+k+1)}\left(\frac{x}{2}\right)^{n+2k} \qquad (4)$$

In order to calculate diffusion coefficient (k) from Equation (3), a computer program was developed. The calculation process uses sixteen α (from α_1 to α_{16}) in Equation (3).

d) Calculation of corrosion initiation time

Generally, it is very difficult to clarify the time at which the corrosion of steel embedded in concrete initiates. In this study, it is assumed that steel corrosion begins at the time when the chloride content in the

mortar reaches a value of 0.4% versus cement weight. This time is calculated based on the chloride ion diffusion coefficient and the surface chloride content [35][36]. Figure 3 shows the calculated corrosion initiation time. As this makes clear, corrosion begins in submerged and tidal zones after about 5 months, and the variation among the different exposure ports is relatively small for the submerged and tidal zones. On the other hand, corrosion in splash zone begins much later, and the variation among exposure locations is greater than in the case of the submerged and tidal zones.

Fig. 3 Calculated corrosion initiation time

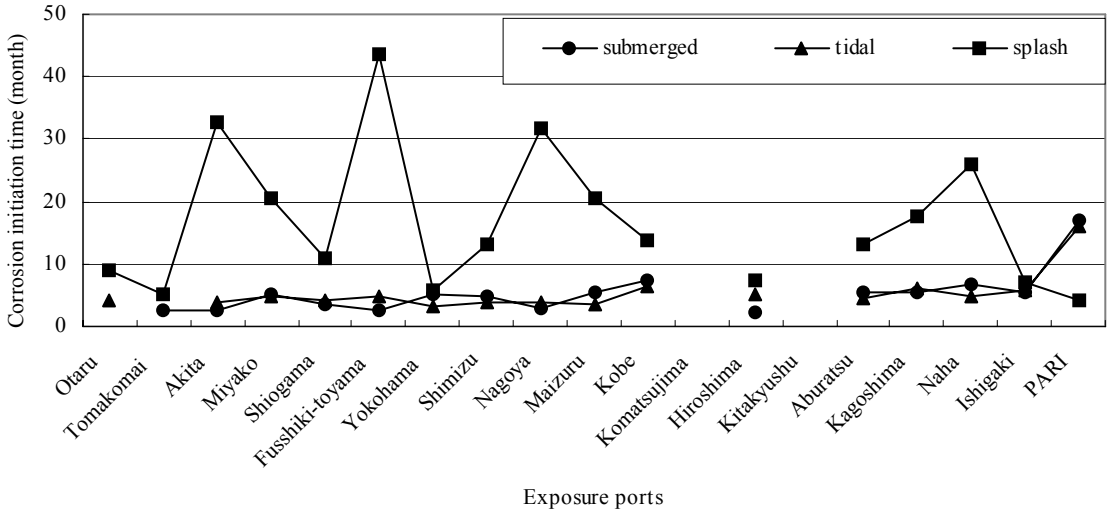

f) Electrical resistance of mortar

The system used to measure the mortar's electric resistance is shown in Fig. 4. Before taking measurements, the specimen was immersed in tap water for 24 hours. As indicated in Fig.4, the resistance between the steel bar and the counter electrode was measured using AC at a frequency of 100 Hz. With this measurement method, the obtained value is actually the sum of the resistance of the mortar and the resistance of tap water. However, the value obtained is treated as the resistance of the mortar. Figure 5 shows the obtained electrical resistance measurements for mortar after 2 years of exposure. The resistance of specimens from the submerged and tidal zones is smaller than that of those from the splash zone and the land zone. Given the link between mortar moisture content and electrical resistance, it can be inferred that the moisture content is greatest in the submerged zone and tidal zone, followed by that in the splash zone and the land zone. In all zones, there is variation among exposure ports, so environmental conditions can be treated as different at each port.

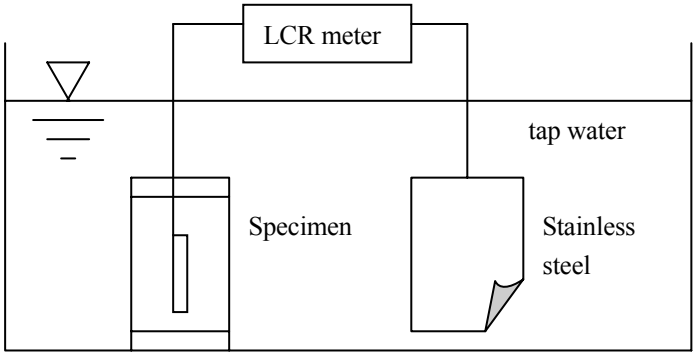

Fig. 4 Measurement of mortar electrical resistance

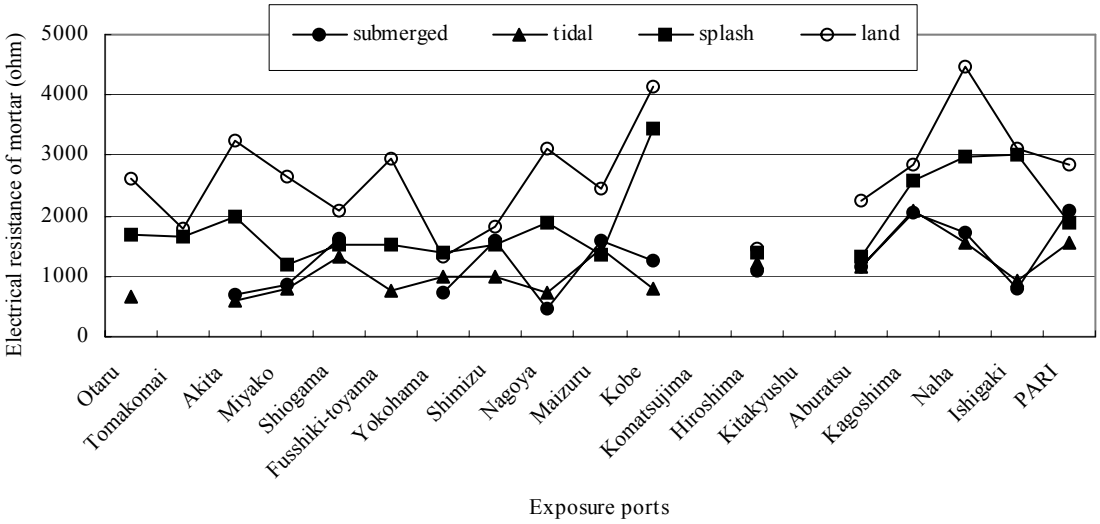

Fig. 5 Electrical resistance of mortar (after 2years of exposure)

g) Polarization resistance of embedded steel bar

Figure 6 shows the system used to measure polarization resistance. This is known as the three-electrode method, and uses a saturated calomel electrode as the reference electrode and stainless steel as the counter electrode. A potentiostat is used for actual measurements, and a function generator is used to generate the signal. Results are recorded using an analogue X-Y recorder. The immersion solution is ordinary tap water.

The measurement procedure is as follows: 1) the specimen is immersed in tap water for 24 hours; 2) the half-cell potential is measured; 3) from the half-cell potential, the potential is swept as [half-cell potential] —> [half-cell potential + 5 mV] —> [half-cell potential - 5 mV] —> [half-cell potential]; 4) the current flow is measured continuously as the potential is swept. The potential sweep rate is 40 mV/s. Polarization resistance is calculated from the current flow at the half-cell potential + 5 mV point. With this linear polarization resistance method, resistance between the working electrode and the counter electrode becomes a factor affecting measurement error. In this study, based on the results of research carried out by one of the authors [37], the error is deduced from the collected data using Equation (5).

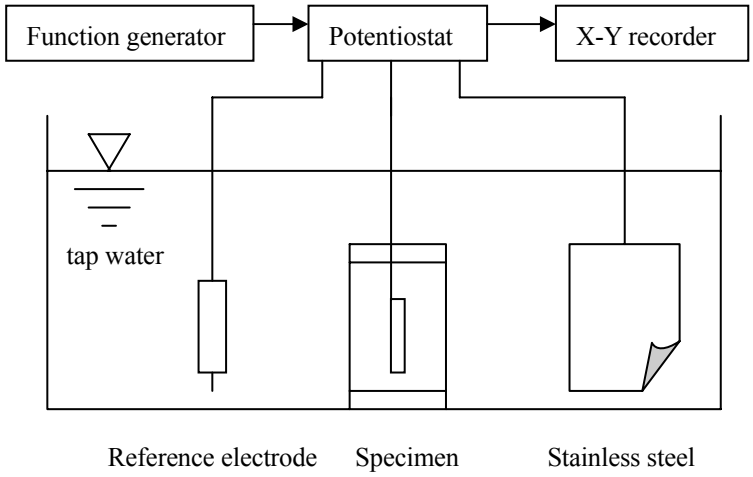

Fig. 6 Measurement of electrochemical measurement

$$x' = x + 0.52 \cdot (1000 - y) \qquad (5)$$

Here, x: measured polarization resistance data, y: electrical resistance of mortar at the time of measurement, and x': corrected value of polarization resistance at a resistance of 1,000 mV. As Equation (5) shows, all data are corrected to values at a resistance of 1,000 mV.

Figure 7 shows the polarization resistance of embedded steel bars measured after 2 years of exposure. Polarization resistance is almost equal for specimens in the submerged and tidal zones, and the values are smaller than those of samples in the splash zone and land zone. The polarization resistance in splash zone, is larger than those of submerged and tidal zones, however, is smaller than that of land zone. This implies

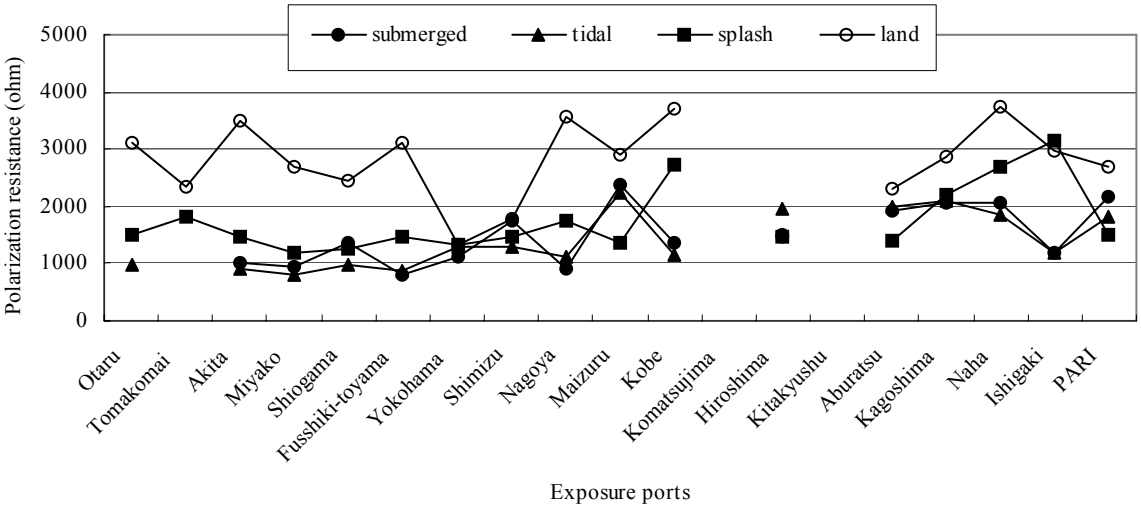

Fig. 7 Polarization resistance (after 2years of exposure)

that steel embedded in mortar specimens in the submerged and tidal zones is much more prone to loss of

passivity than that in specimens in the splash and land zones. The splash zone is a better environment than the submerged and tidal zones, but the land zone is much better yet. In all zones, there is considerable variation among exposure ports, so it is inferred that environmental conditions vary considerably among the ports.

g) Potential-step test (oxygen diffusion test)

The measurement system shown in Fig. 6 is also used for potential-step testing. The specimen was first immersed in ordinary tap water for 24 hours. The subsequent measurement procedure was as follows: 1) the potential of the steel bar was set to 1,000 mV and held constant then 2) the current flowing from the steel was measured continually. Current flow was a maximum when measurements began, gradually falling thereafter until reaching an almost constant value after a period of about 10 hours. Theoretically, this variation in current depends on the supply of oxygen to steel bar in the mortar. According to electro-chemical theory, based on Equation (6) for the oxygen diffusion in mortar (Ficks' 2nd law) and the assumption that the oxygen concentration at the steel surface is zero, the time-current line can be expressed as Equation (7), which is called Cottrells' equation.

$$\frac{\partial C}{\partial t} = D\frac{\partial^2 C}{\partial x^2} \qquad (6)$$

$$I = nFDC\frac{1}{\sqrt{\pi Dt}} \qquad (7)$$

Here, I: current flow (A), n: number of reactive electrons, F: Faraday's constant, D: oxygen diffusion coefficient, C: oxygen concentration at the steel surface just before measurement, and t: time from start of measurement.

Equation (7) shows that the reaction rate at the steel surface (the oxygen consumption rate) is inversely proportional to the square root of t. At a later stage of measurements, after an elapsed time of 10 hours, the current value becomes almost constant. This constant current depends on oxygen diffusion in the mortar specimen.

Figure 8 gives the results of potential-step measurements after 2 years of exposure; this is the current density (current value divided by steel area) after an elapsed time of 10 hours. The variation among exposure ports is almost the same for submerged zone and tidal zone specimens, and also between splash zone and land zone specimens. The average value for the splash zone is larger than that of the submerged and tidal zones, but is smaller than that of land zone. Thus the overall trend seen in this potential-step test is similar to that of electrical resistance, which was shown in Fig. 5. It is inferred that the electrical resistance of the mortar correlates with the results of the potential-step test.

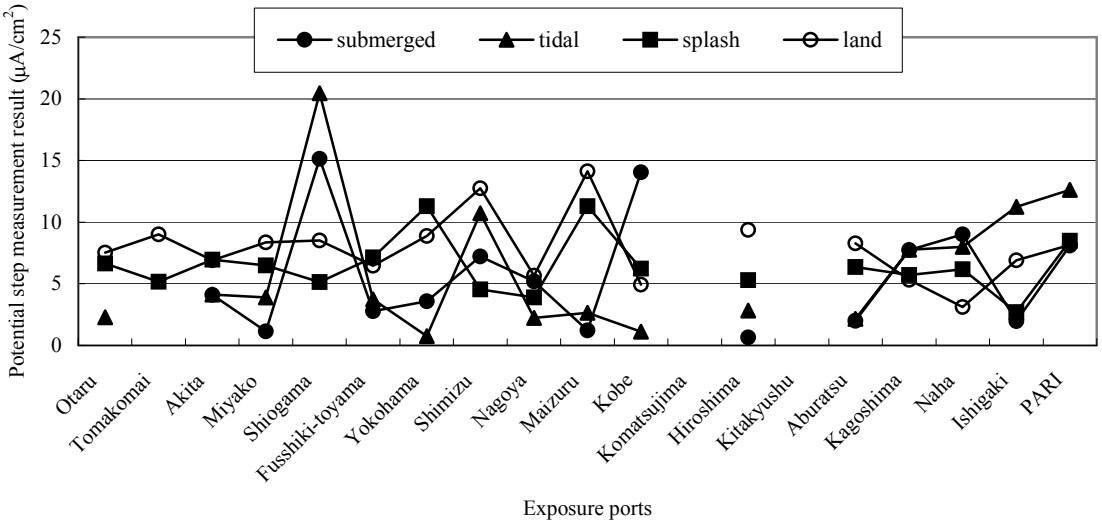

Fig. 8 Potential-step measurements (after 2years of exposure)

h) Corroded area test

After tests above b) - g) had been completed, each mortar specimen was sliced open and the steel bar removed. Visual observations of the steel bar were made immediately, and the surface was sketched. From the sketch, the corroded area was calculated. Here, "corroded area" is defined as the ratio of corroded area to total surface area. Figure 9 shows the corroded area of the specimens. Specimens exposed in the tidal zone have the largest corroded area, followed by those in the submerged zone, the splash zone, and the land zone in that order. In the submerged and tidal zones, specimens exposed in relatively cold climates have relatively larger corroded area. However, in the splash zone, there is little difference among exposure

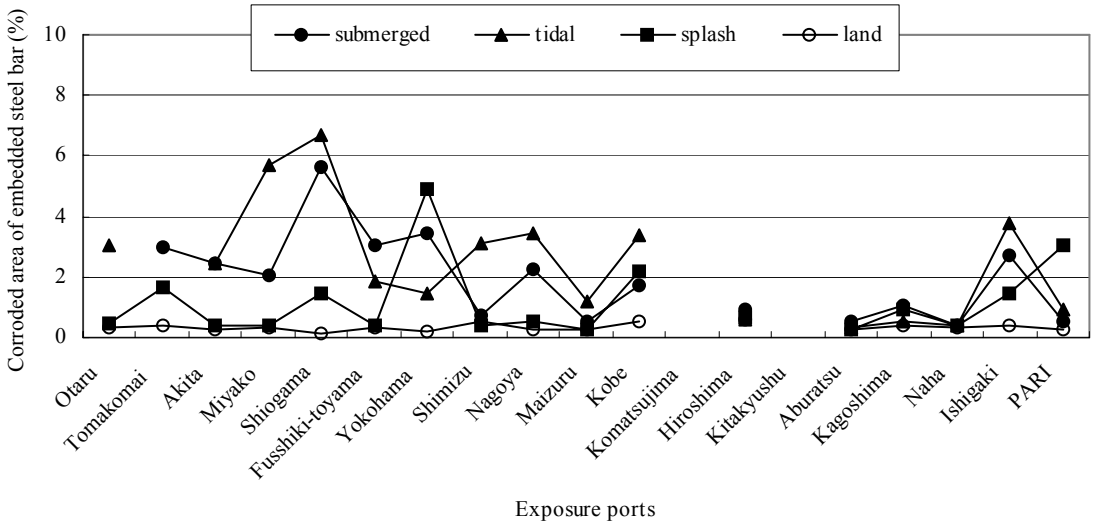

Fig. 9 Corroded area of embedded steel bar (after 2years of exposure)

ports. In the land zone, the corroded area is very small for all ports, and again there is no clear difference

among exposure ports.

3. SELECTION OF ENVIRONMENTAL PARAMETERS

3.1 Seawater Analysis at Exposure Ports

Table 4 presents the coefficient of interrelationship between each parameter of seawater chemical characteristics. There is no apparent relationship between specific gravity and other parameters. However, there is a relationship between pH value and other parameters (0.75 - 0.85). There is also a clear relationship among the chemical components. Of the six components measured, chloride ion concentration is selected as a parameter representative of seawater chemical content. Thus specific gravity, pH, and chloride ion concentration are selected as parameters representing seawater characteristics in the analysis that follows.

Table 4 Coefficient of interrelationship between each parameter of seawater chemical characteristics

	pH	Seawater chemical compositions					
		Na	K	Ca	Mg	Cl^-	SO_4
Specific gravity	-0.32	-0.10	-0.09	-0.08	-0.04	-0.09	-0.09
pH		0.82	0.83	0.79	0.76	0.83	0.82
Na			0.99	0.99	0.99	1.00	1.00
K				0.97	0.98	1.00	1.00
Ca					0.99	0.98	0.98
Mg						0.98	0.98
Cl^-							1.00

3.2 Climatic and Wave Conditions at Exposure Ports

a) Correlation with climatic conditions

Table 5 presents coefficients of interrelationship for each climatic factor. There is good correlation between average temperature and average maximum temperature, and also between average wind velocity and maximum wind velocity. Therefore, as representative climate parameters, average temperature and average wind velocity are selected. For the analysis that follows, five climatic parameters are selected: 1) average temperature, 2) humidity, 3) sunshine hours, 4) amount of rainfall, and 5) average wind velocity; one additional parameter is also used: 6) temperature difference. Here, temperature difference is the absolute

Table 5 Interrelationship coefficients among climate conditions

		Temperature	Humidity	Wind velocity		Sunshine hours	Amount of rainfall
		Max.		Ave.	Max.		
Temperature	Ave.	0.99	-0.26	0.59	0.44	0.27	0.61
	Max.		-0.31	0.51	0.39	0.29	0.63
Humidity				0.02	-0.05	-0.50	0.02
Wind velocity	Ave.				0.92	0.28	0.37
	Max.					0.22	0.29
Period of sunshine							0.15

value of the difference between the temperature at each port and the average value for all ports. This parameter is added so as to enable evaluation of cold climate areas and hot areas under similar conditions.

b) Correlation between climatic conditions and seawater composition

Table 6 presents the coefficient of interrelationship between climatic conditions and seawater characteristics. There is no obvious correlation between the two.

Table 6 Interrelationship coefficients between climatic conditions and seawater characteristics

		Average temperature	Average humidity	Average wind velocity	Period of sunshine	Amount pf rainfall
Characteristics of seawater	Specific gravity	0.11	-0.27	-0.15	0.36	-0.02
	PH	0.55	-0.06	0.19	-0.07	0.22
	Cl^-	0.33	0.00	0.07	0.11	-0.08

c) Correlation between climatic conditions and wave conditions

Wave motion is normally caused by the wind, so the governing factors of wave height are wind velocity and fetch. Figure 10 shows the correlation between wave data (wave height divided by wave period) and climatic data (wind velocity). There is a good relationship between wave data and climatic data. Thus, wind velocity is selected as representative of wave conditions in the analysis that follows.

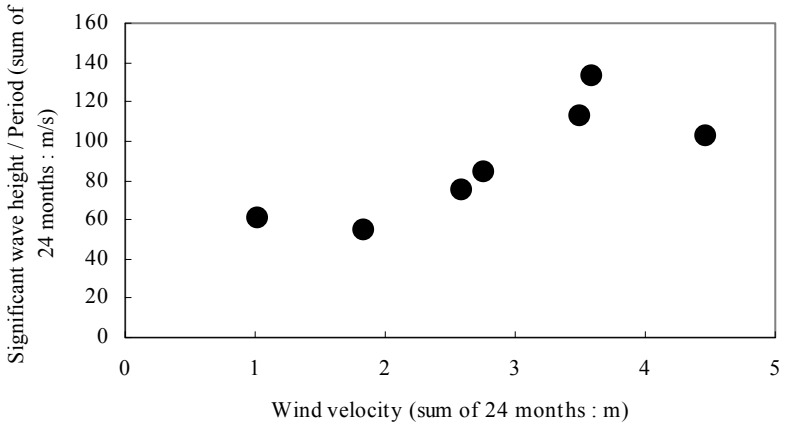

Fig. 10 Correlation between wave data and climate data

3.3 Analysis Procedure

Figure 11 shows the analysis procedure. First, the data are normalized using the z-point conversion. This involves fitting all data into a distribution with an average of “0” and a standard deviation of “1”. Next, applying principal component analysis to all the data, the main parameters are selected from among all parameters. Finally, multiple regression analysis is carried out on the several selected main parameters. Based on the results of this multiple regression analysis, the relationship between corrosion of steel in the concrete and environmental conditions is discussed.

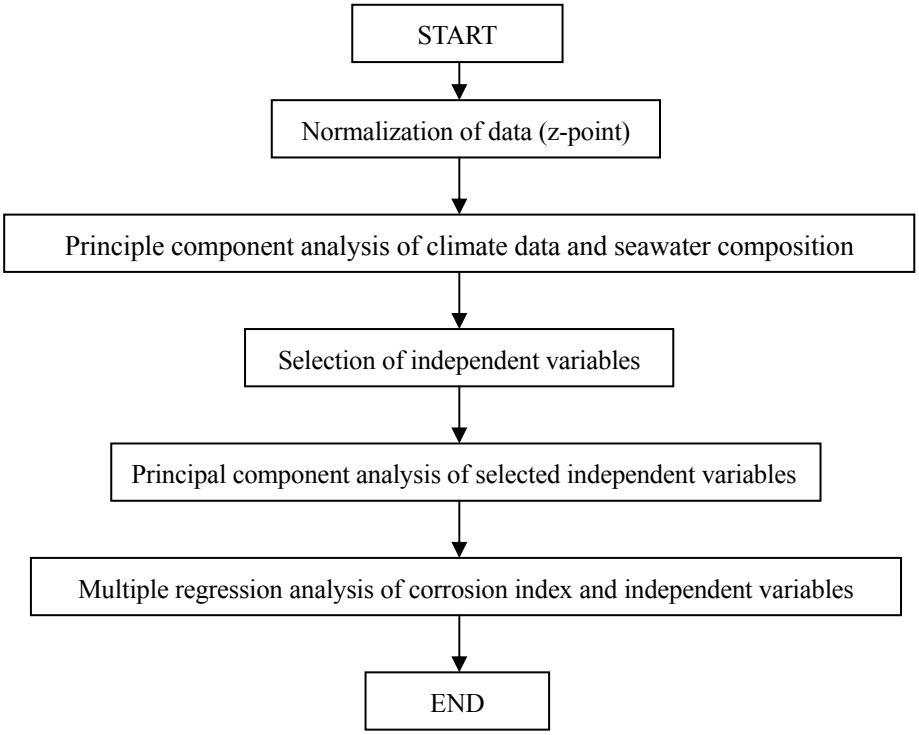

Fig. 11 Multiple variable analysis procedure used in this study

a) Principal component analysis

This analysis is carried out on nine factors, consisting of seawater characteristics (pH, chloride ion concentration, specific gravity) and climatic conditions temperature, temperature difference, humidity, wind velocity, sunshine hours, amount of rainfall).

b) Principal component analysis results

Figures 12 and 13 show the results of principal component analysis. In Fig. 12, the x-axis represents the first principal component and the y-axis is the second principal component. In Fig. 13, the x-axis represents the first principal component and the y-axis the third principal component. In the figures, the nine factors are categorized into several groups that exhibit similar trends. For example, the climatic factors, such as amount of rainfall and wind velocity are grouped together with the seawater characteristics pH value and chloride ion concentration. On the other hand, humidity and sunshine hours have the opposite effect to this grouping, so it can be said that they also belong to one group. Based on these analysis results, the following five factors are selected for the subsequent multiple regression analysis:

1) Chloride ion concentration in seawater, as a representative of seawater conditions
2) Wind velocity, as a representative of wind and wave conditions
3) Temperature, as a representative of temperature
4) Temperature difference, as a representative of regional climate (hot or cold)
5) Humidity, as a representative of dry/wet conditions

1 Sunshine hours　2 Amount of rainfall　3 Wind velocity　4 Temperature　5Humidity
6 Temperature difference　7 pH　8 Chloride concentration　9 Specific gravity

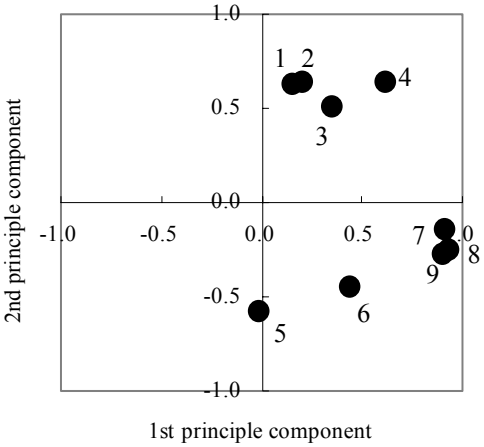

Fig. 12 Two-dimensional expression of analysis results (1st and 2nd principal components)

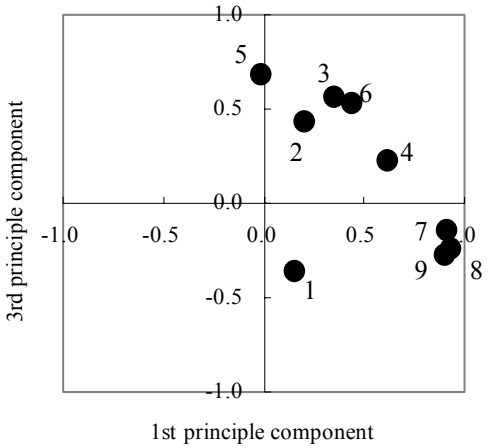

Fig. 13 Two-dimensional expression of analysis results (1st and 3rd principal components)

4. ANALYSIS OF RELATIONSHIP BETWEEN ENVIRONMENTAL CONDITIONS AND MORTAR SPECIMEN PROPERTIES

4.1 Method of Multiple Regression Analysis

This study adopts the analysis model expressed by Equation (8).

$$y_i = a_{i1} \cdot x_1 + a_{i2} \cdot x_2 + a_{i3} \cdot x_3 + a_{i4} \cdot x_4 + a_{i5} \cdot x_5 + b_i + \varepsilon \qquad (8)$$

Here, y_i: experimental result obtained from mortar specimen, X_1: chloride ion concentration of seawater X_2: wind velocity, X_3: temperature, X_4: humidity, X_5: temperature difference, a_{i1} - a_{i5}: regression coefficients, bi: constant (=0 for analysis using normalized data), ε: error.

The computer program used for this analysis is "SPSS", as used also for the principal component analysis. The model with the highest multiple correlation coefficient is treated as the best fit model.

4.2 Multiple Regression Analysis with Corrosion Initiation Time as Criterion Variable

Tables 7 and 8, and Fig. 14 present the results of analysis with corrosion initiation time as the criterion variable. For the tidal zone, temperature and wind velocity affect the corrosion initiation time. For the submerged, tidal, and splash zones, temperature affects corrosion initiation time, with lower temperatures (i.e. cold winter conditions) resulting in earlier corrosion initiation. For both the tidal and splash zones, wind velocity has an effect on corrosion initiation time, with higher wind velocities leading to earlier

corrosion initiation. Furthermore, both for the submerged and splash zones, the chloride concentration of the seawater affects corrosion initiation time. However, the effect is completely different for the two cases; in the submerged zone, the lower the chloride concentration, the earlier corrosion begins. However, in the splash zone, higher chloride concentrations result in earlier corrosion initiation times.

Table 7 Multiple regression analysis results with corrosion initiation time as criterion variable
-- Normalized multiple correlation coefficient --

	Submerged zone	Tidal zone	Splash zone
Cl^- concentration of seawater	0.371	0.075	-0.894
Temperature	0.589	0.537	0.631
Temperature difference	-0.218	0.326	0.185
Humidity	0.093	-0.327	0.190
Wind velocity	-0.152	-0.436	-0.510

Table 8 Multiple regression analysis results with corrosion initiation time as criterion variable

Environment	Multiple regression equation
Submerged zone	Y=0.444*(temperature)+0.320*(Cl^- concentration of seawater) R*=0.311, R=0.640
Tidal zone	Y=0.683*(temperature)-0.401*(wind velocity) R*=0.168, R=0.536
Splash zone	Y=0.598*(temperature)-0.811*(Cl^- concentration of seawater) -0.442*(wind velocity)+0.260*(humidity) R*=0.479, R=0.786

R*: multiple correlation coefficient adjusted for the degree of freedom
R: multiple correlation coefficient

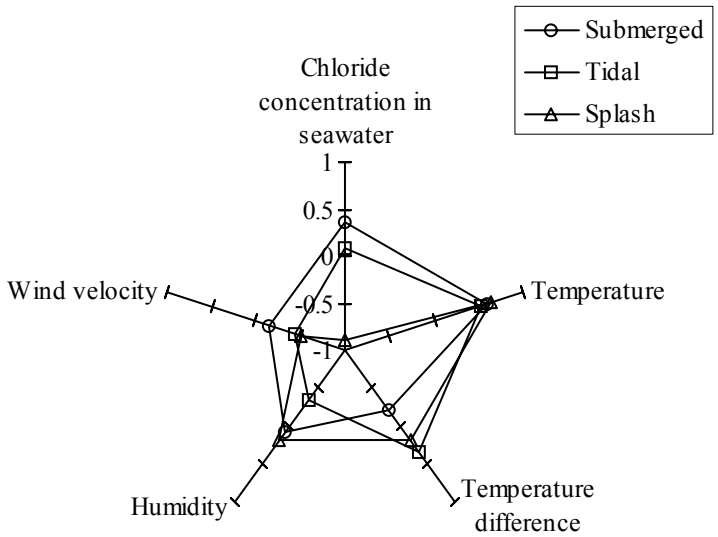

Fig. 14 Rader chart showing standard coefficient of corrosion initiation time

4.3 Multiple Regression Analysis with Polarization Resistance as Criterion Variable

Tables 9 and 10, and Fig. 15 present the results of analysis with polarization resistance as the criterion variable. For the splash zone, temperature affects the corrosion rate. As Fig. 15 shows, environmental conditions in the tidal zone are intermediate between those in the submerged zone and in the splash zone.

Table 9 Multiple regression analysis results with polarization resistance as criterion variable

-- Normalized multiple correlation coefficient --

	Submerged zone	Tidal zone	Splash zone
Cl^- concentration of seawater	-0.669	-0.494	0.141
Temperature	-0.144	-0.467	-0.662
Temperature difference	0.562	0.538	-0.626
Humidity	-0.195	-0.007	0.345
Wind velocity	-0.414	-0.111	0.232

Table 10 Multiple regression analysis results with polarization resistance as criterion variable

Environment	Multiple regression equation
Submerged zone	Y=-0.691*(Cl^- concentration of seawater)+0.422*(temperature difference)-0.423*(wind velocity) R*=0.358, R=0.712
Tidal zone	Y=-0.460*(Cl^- concentration of seawater)+0.504*(temperature difference)-0.539*(temperature) R*=0.502, R=0.780
Splash zone	Y=-0.622*(temperature) R*=0.479, R=0.786

R*: multiple correlation coefficient adjusted for the degree of freedom

R: multiple correlation coefficient

Fig. 15 Rader chart showing regression coefficient of polarization resistance

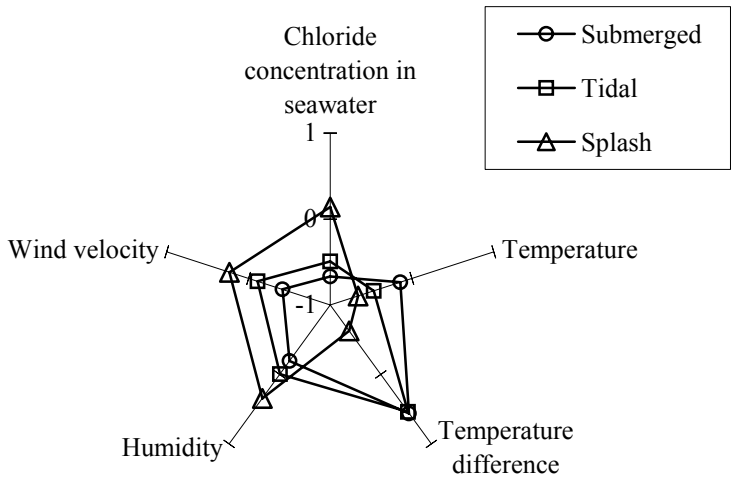

In all zones, the chloride ion concentration and temperature difference have a relatively large effect on corrosion rate. The lower the chloride concentration in the seawater, the greater the corrosion rate. And, the larger the temperature difference, the greater the corrosion rate is. This means that in areas with

temperature extremes, the corrosion rate is much larger than in areas with more moderate temperature variations. On the other hand, in the tidal and splash zones, the actual temperature has an effect on corrosion rate, with lower temperatures resulting in larger corrosion rates. Generally speaking, these test results contradict electrochemical theory as regards the relationship between reaction rate and temperature. However, in this two-years exposure test, the effect of freeze-thaw cycles on the deterioration of mortar specimens is not evaluated, and there is a possibility that the results come about because of freeze-thaw action on mortar specimens.

4.4 Analysis of Potential-step Test Results

Tables 11 and 12,and Fig. 16 present the results of analysis with the potential-step test results as the criterion variable. For the submerged zone, it was impossible to obtain a best-fit model. This means that no environmental condition was found in the study that affects oxygen diffusion in concrete in the submerged zone. Table 11 and Table 12 clarify that humidity has an effect in both the tidal and splash zones, with higher humidity resulting in larger oxygen diffusion coefficients. In the tidal zone, wind velocity also has an effect on oxygen diffusion in mortar specimens, higher the wind velocity is, larger the oxygen diffusion coefficient is. On the other hand, in the splash zone, temperature difference has an effect on oxygen diffusion coefficient, with a smaller temperature difference resulting in a higher oxygen diffusion coefficient.

Table 11 Multiple regression analysis results with potential-step test results as criterion variable

-- Normalized multiple correlation coefficient --

	Submerged zone	Tidal zone	Splash zone
Cl^- concentration of seawater	Not available	0.149	0.259
Temperature	Not available	-0.099	-0.106
Temperature difference	Not available	-0.023	-0.567
Humidity	Not available	0.559	0.255
Wind velocity	Not available	0.365	-0.141

Table 12 Multiple regression analysis results with potential-step test results as criterion variable

Environment	Multiple regression equation
Submerged zone	Not available
Tidal zone	Y=0.562*(humidity)+0.312*(wind velocity) R*=0.316, R=0.643
Splash zone	Y=0.281*(humidity)-0.512*(temperature difference) R*=0.095, R=0.464

R*: multiple correlation coefficient adjusted for the degree of freedom

R: multiple correlation coefficient

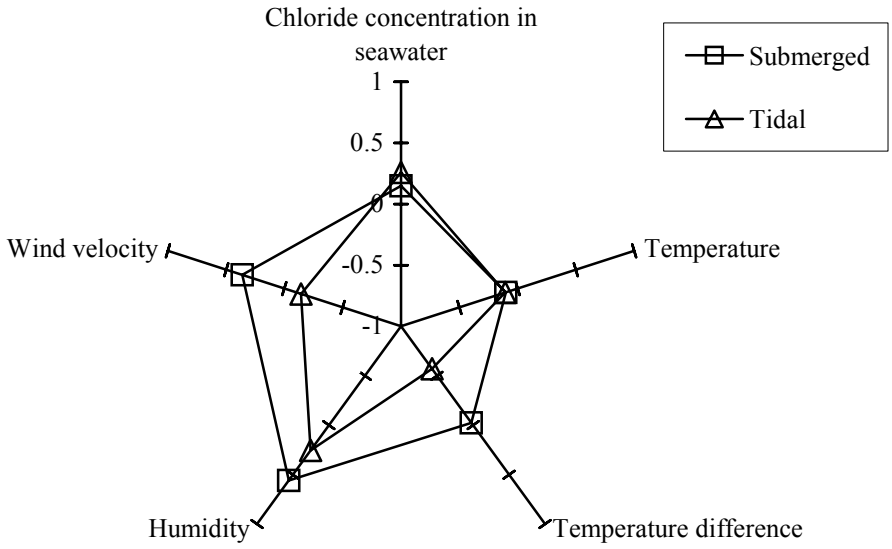

Fig. 16 Rader chart showing regression coefficient of potential-step measurement results

5. CONCLUSIONS

In this study, exposure tests of small mortar specimens were carried out at nineteen Japanese ports in order to determine which environmental conditions affect the corrosion of steel embedded in concrete. Based on the analysis of the exposure test results, the following conclusions have been derived:

1) Five factors are selected as the main parameters affecting chloride-related deterioration of RC structures in a marine environment, as follows: 1) chloride ion concentration in the sea water, 2) wind velocity, 3) temperature, 4) temperature difference, and 5) humidity.

2) In the submerged, tidal, and splash zones, temperature has an effect on corrosion initiation time, with lower temperatures resulting in earlier corrosion initiation. Further, in the tidal and splash zones, wind velocity has an effect on corrosion initiation time, with higher wind velocities (that is, rougher wave conditions) leading to earlier corrosion initiation.

3) In the submerged and tidal zones, both chloride ion concentration and temperature difference have an effect on the steel corrosion rate, with lower chloride ion concentrations leading to higher corrosion rates. Also, greater temperature differences result in higher corrosion rates. Further, in the tidal and splash zones, temperature has an effect on the steel corrosion rate, with lower temperatures resulting in higher corrosion rates.

4) Humidity conditions around the concrete have a great effect on oxygen diffusion within the concrete, both in the tidal and splash zones. Higher humidity levels result in higher oxygen diffusion coefficients.

5) Concerning corrosion initiation time and corrosion rate, environmental conditions are much more severe in areas with a cold climate within the scope of this study.

References

[1] Nobuaki Otsuki, Deterioration Condition of Port Structures, JCI Concrete Journal, Vol.25, No.11, pp.63-67, 1987. (in Japanese)
[2] Nobuaki Otsuki, Masamitsu Haramo and Hidenori Hamada, Outline Survey on Deterioration of Concrete of Wharf Structures, Technical Note of the Port and Harbour Research Institute, No.617, June 1988. (in Japanese)
[3] Nobuaki Otsuki, Masamitsu Haramo and Hidenori Hamada, Detailed Survey on Deterioration of Concrete of Wharf Structures, Technical Note of the Port and Harbour Research Institute, No.627, Sept. 1988. (in Japanese)
[4] Nobuaki Otsuki, Research on the Influence of Chloride on Corrosion of the Embedded Steel Bars in Concrete, Report of the Port and Harbour Research Institute, Vol.24, No.3, Sept. 1985. (in Japanese)
[5]-[28] Monthly Report of Japan Meteorological Agency, October 1989 – September 1991. (in Japanese)
[29] Koji Kobune, Yutaka Kameyama, Norihiko Nagai, Kazuaki Sugawara and Noriaki Hashimoto, Annual Report on Wave Properties at the Network Stations (1989), Technical Note of the Port and Harbour Research Institute, No.712, June 1991. (in Japanese)
[30] Norihiko Nagai, Kazuaki Sugawara, Noriaki Hashimoto, Tadashi Asai and Takayuki Hirano, Annual Report on Wave Properties at the Network Stations (1990), Technical Note of the Port and Harbour Research Institute, No.721, Mar. 1992. (in Japanese)
[31] Norihiko Nagai, Kazuaki Sugawara, Noriaki Hashimoto and Tadashi Asai, Annual Report on Wave Properties at the Network Stations (NOWPHAS, 1991), Technical Note of the Port and Harbour Research Institute, No.745, Mar. 1993. (in Japanese)
[32] JCI Standard (draft) on Test Methods related to Corrosion and Corrosion Prevention of Concrete Structures, Japan Concrete Institute, 1987. (in Japanese)
[33] Jiro Kondo, Iwaro Takahashi, Ryuichi Kobayashi, Yoshio Koyanagi and Tadashi Watanabe, Differential equation and Fourier analysis, Baifukan, 1981. (in Japanese)
[34] Brown R. D., Mechanism of Corrosion of Steel in Concrete in Relation to Design, Inspection and Repair of Offshore and Coastal Structures, Performance of Concrete in Marine Environment, ACI SP65, 1980.
[35] Hidenori Hamada and R. N. Swamy, A Discussion on Chloride Ingress into Concrete under Various Marine Environments, JCI Concrete Research and Technology, Vol.7, No.1, Jan. 1996. (in Japanese)
[36] Hidenori Hamada and R. N. Swamy, A Discussion on Chloride Ingress into Concrete under Various Marine Environments, Technical Note of the Port and Harbour Research Institute, No.810, Sept. 1995. (in Japanese)
[37] Hidenori Hamada, Tsutomu Fukute, Hiroshi Yokota and Masami Abe, Fundamental Study on the Effectiveness of Concrete Resistance on Linear Polarization Resistance Measurements, Proceedings of Annual Conference Held by The Society of Materials Science, Japan, 1997.9. (in Japanese)
[38] Hideaki Kita and Kohei Uosaki, Electro-chemistry, Gihodo-syuppan, 1983. (in Japanese)
[39] Shoji Sato and Yoshimi Goda, Coastal and Port Engineering, Shokoku-sya, 1972.3. (in Japanese)
[40] Syuichi Shinmura, Data Analysis Using Personal Computer, Kodan-sya, 1995.11. (in japanese)
[41] Yutaka Tanaka, Tomoyuki Tarumi and Kazumasa Wakimoto, The 2nd Handbook on Statistics Using Personal Computer (Multiple variable analysis), Kyoritsu-syuppan, 1984.9. (in Japanese)